MEMS RELAYS FOR POWER SWITCHING APPLICATIONS

A. C. Weber[1], A. H. Slocum[2], and J. H. Lang[2]
[1]FormFactor Inc., Livermore, CA, USA
[2]Massachusetts Institute of Technology, Cambridge, MA, USA

Abstract: This paper presents the design, modeling, fabrication and testing of MEMS relays for make-break power switching applications. The relays feature {111}-plane silicon etched electrical contacts with electro-deposited refractory metal surfaces such as alloyed Pd and Rh. A 50-μm standoff across two series air gaps provides 1-kV electrical isolation in air at atmospheric pressure, tested to 970 V. Electrostatic zipper actuators provide a minimum contact resistance of 130 mΩ, and a maximum ampacity of 0.8 A, tested for 10^5 cycles. The MEMS relays are fabricated in (100) Si through deep reactive ion etching (DRIE), crystalline-orientation-dependent etching using KOH, electroplating of the contacts, and anodic bonding to a glass handle.

Keywords: {111} Si etched contacts, KOH etching, DRIE, zipper electrostatic actuators, make-break MEMS switch, electro-deposition.

INTRODUCTION

Unlike solid-state devices, mechanical relays provide galvanic isolation between their control and power ports. Electrical safety codes require loads in certain power-system applications to be disconnected by open gaps. Typical power relays have off-state voltages on the order of 360 V [1] or below, while telecom relays may be subject to surges of up to 2.5 kV and several A [2]. Surface electroplated contacts with electrostatic actuation can exhibit 30-mΩ contact resistance and a maximum on-state current, or ampacity, of 1-2 A, but have an open gap of only 3 μm which limits the stand-off voltage to the Paschen minimum of 330 V in air at atmospheric pressure [3], or lower if arcing occurs across dielectric layers. Power relays with larger ampacity (3 A) and larger open gaps (100 μm) exist. However, they also exhibit much higher contact resistances (100-1300 mΩ) [4,5]. MEMS relays with lateral displacement contacts typically offer gaps of 10-100 μm and contact resistances of tens of Ω [5,6]. One such relay with electroplated Au contacts has maintained a contact resistance of 10 mΩ for 10^9 cycles [7] while cold switching. However, its structural material is SU-8, making it unsuitable for power switching applications because of the material thermal and structural properties. The objective of this research is to develop a MEMS relay capable of reliably hot-switching currents on the order of 1 A, and providing galvanic isolation in excess of 1 kV.

DESIGN

To achieve reliable operation, 1-A on-state ampacity and 1-kV off-state isolation, the following functional requirements must be met. The contact stand-off must exceed 76 μm across a single air gap at atmospheric pressure, as expressed by Paschen's law [8,9]. The relay must exert sufficient closing and opening forces to provide a reliable contact resistance and to overcome contact adhesion. For example, a minimum closing force of 0.1-0.6 mN and 5-10 mN is required to achieve stable and low contact resistance with soft (Au) and refractory (Ru) metal contacts, respectively [10]. A minimum opening force of 0.1-2.7 mN is required to overcome contact adhesion [10]. Contact wipe is desired to increase contact reliability as friction is known to help break through isolating oxide and organic films. Contact materials with high melting temperatures are preferred over soft metals [2] for enhanced reliability.

For these requirements, a single pole, single-throw, metal-contact MEMS relay is designed with {111} Si etched electrical contacts [11,12] as shown in Figure 1. These contacts consist of parallel {111} silicon surfaces created by sequentially etching two back-to-back, offset, self-terminating V-grooves into a (100) 300-μm-thick Si substrate using KOH solution. The oblique geometry of the {111} contacts results in more uniform and thicker metallization due to the larger projected area during evaporation which results in lower path resistance. The {111} Si etched contacts introduce contact wipe, which increases contact reliability. The relay uses two 50-μm air gaps in series to provide an effective 100 μm standoff. The excess standoff accounts for field enhancement effects.

The MEMS relay, shown in Figure 1, comprises a single silicon device layer micromachined with DRIE and KOH etching. The device layer is bonded to a glass handle which provides mechanical support and electrical isolation. The relay has a compliant mechanism comprising four double parallelogram flexures (1), eight pairs of zipper [13] electrostatic

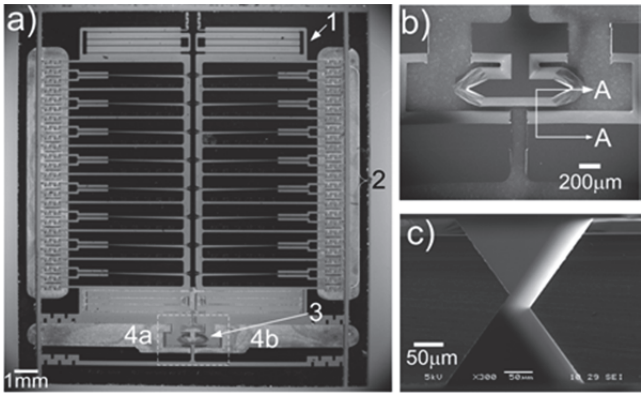

Figure 1. Fabricated MEMS relay. Die top view (a); contact detail, prior to metal deposition (b); contact cross section A-A, as shown in Figure 1b, without the metal film for clarity (c).

actuators (2) which provide in-wafer plane actuation for closing and opening, a moving {111} Si etched contact (3), and two static {111} Si etched contacts (4a,b). The {111} contacts [11,12] are electroplated with a 10-µm thick buffer layer of either Ni or Cu, and a 2-µm thick refractory metal such as alloyed Pd or Rh.

FABRICATION

Figure 2 shows the MEMS relay fabrication process. The device layer is etched in (100) Si using deep reactive-ion etching (DRIE) and crystalline-orientation-dependent KOH etching with nested silicon-dioxide and silicon-nitride masks (a-k). A Au seed layer is evaporated through a shadow wafer onto both sides of the device wafer (l), and the device layer is bonded to a glass substrate (m). Conductive metal films are next electroplated over the seed layer onto the contacts, starting with a buffer layer of Cu or Ni covered by a 2-µm thick refractory metal such as alloyed Pd or Rh. After electro-deposition, the device is released by dicing through the device layer, and wire-bonded to a pin grid array IC package for testing.

MODELING

The theoretical ampacity of the MEMS relay is derived from a mechanical, electrical and thermal model. The model is based on a self-heated resistor with temperature-dependent electrical resistivity operating at constant current [14]. Plastic deformation contact mechanics is first used to determine the electrical contact radius a, or "a-spot", and the contact resistance as functions of the actuation force and temperature. Next, the electrical contact radius a is used to determine the thermal contact radius b. Finally, a thermal model determines the temperature

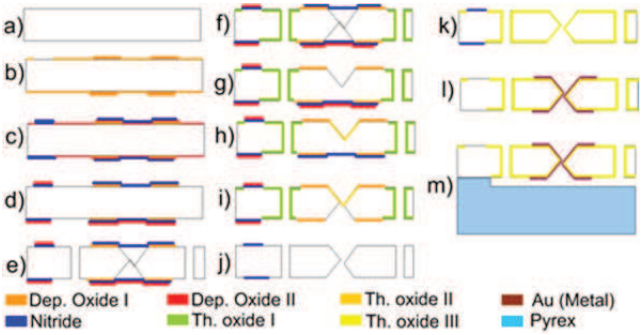

Figure 2. Schematic of the MEMS relays fabrication process prior to electro-deposition of the electrical contacts.

rise of the constriction caused by steady-state Joule heating. The ampacity, defined here as the current that causes thermal runaway, follows directly.

The electrical constriction resistance R_c, or contact resistance, of two mono-metallic surfaces in mechanical contact is given by the Maxwell equation

$$R_c = \rho_e / 2a \tag{1}$$

where ρ_e is the electrical resistivity of the contact material, and a is the electrical contact spot, or a-spot, radius [15,16].

Alternatively, when subject to high contact pressures which cause plastic deformation, the constriction resistance is given by

$$R_c = \sqrt{\rho_e{}^2 \eta \pi H / 4F} \tag{2}$$

where ρ_e is the electrical resistivity of the contact material, H is the material hardness, F is the force exerted on the contacts, and η is an empirical number of order unity [15,16]. By equating (1) and (2) the contact radius is determined as a function of the closing force and of the contact material properties. This contact radius a is used later in the analysis to determine the thermal contact area b. Figure 3 shows the electrical constriction resistance as a function of actuation force for the materials described in Table 1.

Surface asperities also cause a thermal resistance in the system. It is known that the size of the thermal contact area typically exceeds the area of ohmic contact as contamination on the contacts have better thermal conductivity than electrical conductivity.

The steady-state temperature rise (T_s -T_0) of a self-heated resistor under constant current [14] is

$$T_s - T_0 = (R_0 R_t I^2)/(1 - \alpha_r R_0 R_t I^2) \tag{3}$$

where R_0 is the electrical resistance at reference

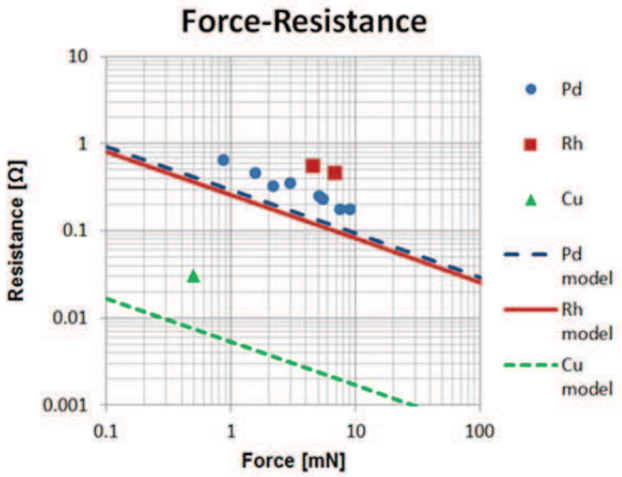

Figure 3. Modeled and experimental force-resistance characteristics of the MEMS relay. Cu data from [3]

temperature T_0, R_t is the thermal resistance to ambient, I is the current, and α_r is the thermal coefficient of resistance. At high currents, $T_s - T_0 \rightarrow \infty$ in (3), and the device experiences thermal runaway. This condition is explained by a rapid decrease in thermal conductivity and a slow increase in electrical resistance as the temperature of the resistor increases.

Consider the steady-state conductive heat transfer model of a joule heated a-spot in a semi-infinite body shown in Figure 4. For simplicity, the temperature inside the heat source of radius b is assumed uniform at T_s. The thermal resistance R_t between the heat source ($r = b$) and the thermal sink ($r = r_0$) [17] is

$$R_t = b\, r_0 / 2\pi k (r_0 - b) \qquad (4)$$

where k is the thermal conductivity, b is the thermal contact radius, which is known to exceed the a-spot size in an electrical contact [15,16] and r_0 is the contact depth beyond which the temperature is assumed to remain constant. The following boundary conditions (BC) are used in (4) to bound the solution. For BC-1, the heat source radius b equals the a-spot radius a and the thermal heat sink radius r_0 is 10 a. BC-1 represents the extreme of completely clean contacts. For BC-2, the heat source radius b is 10 times the a-spot radius a, and the thermal heat sink radius r_0 is 100 a. BC2 represents the presence of contamination. Figure 5 shows the current at thermal runaway conditions for the material properties shown in Table 1 and for the boundary conditions described above. Equation (4) predicts that an ampacity in excess of 1 A is possible with Cu contacts at contact forces F ≥ 0.02 mN, and with Rh and Pd at contact forces of F ≥ 10 mN.

	H[GPa]	ρ[μΩ-cm]	α_r[1/K]	k[W/mK]
Cu	0.125	1.7	4.3e-3	401
Pd	2.87	13.75	3.8e-3	71.8
Rh	9.75	4.9	4.4e-3	88

Table 1. Material properties used in models [17].

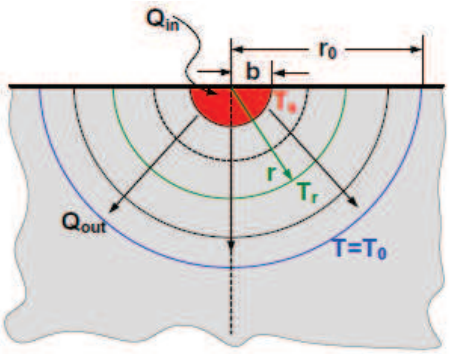

Figure 4. Thermal steady-state conduction model with heat generation.

Notice that the same performance is expected for alloyed Pd and Rh contacts because the differences in resistivity and hardness compensate each other in (2). The similarity in performance between Rh and Pd is confirmed experimentally.

CHARACTERIZATION

The MEMS relay is characterized for force, resistance, on-state ampacity and off-state isolation. The ampacity is determined under continuous switching conditions. The current is increased until relay misses a switching event, which in all cases is caused by contact sticking. The experimental force-resistance and force-ampacity characteristics are shown in Figures 3 and 5, respectively. The experimental forces are estimated from the relay dimensions as fabricated.

In Figure 3, the experimental contact resistance exhibits the same slope as the model. However, the experimental contact resistance is greater than those modeled. This is likely due to the formation of isolating layers on the metal contacts such as organic films, oxides, and frictional polymers, by uncertainty in the material properties, by uncertainty in the estimated forces and/or by limited scrub.

In Figure 5, the experimental data for MEMS relays with alloyed Pd and Rh contacts is in very good agreement with the model with the application of BC-2. However, the experimental data for Cu contacts [3], is over-estimated by almost one order of magnitude. This may be caused by an incorrect boundary condition applied to the Cu contacts. This hypothesis is consistent with the fact that Cu is more

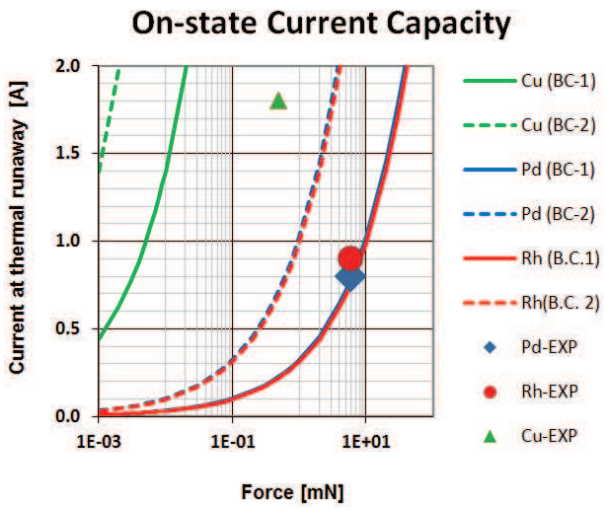

Figure 5. Modeled and experimental force-on state current characteristics of the MEMS relay for two boundary conditions. Cu data from [3].

reactive than Pd and Rh and therefore will result in a higher b/a ratio.

Notice that the thermal model assumes mono-metallic contacts and neglects the electrical and thermal effects of the underlying metal buffer layer of Cu or Ni. For example, from (1), the a-spot size of a 250 mΩ constriction resistance in Pd and Rh is 278 nm and 151 nm, respectively, which is a fraction of the refractory metal thickness used in the contacts (2μm). Thus it is adequate to use a thermal model that considers only the refractory metal and not the underlying buffer metal. Other research points out that under similar circumstances the effect on ampacity of the underlying metal thickness is small and can therefore be ignored [18].

CONCLUSIONS

The use of {111} Si etched contacts can greatly improve ampacity, isolation and the reliability of MEMS relays for power switching applications. The off-state voltage and on-state ampacity of the MEMS relay presented here are compared to other MEMS relays in Figure 6. The oblique geometry of the {111} contacts enables thicker and more uniform metal deposition because of the increased projected area which results in lower path resistance. The {111} contacts introduce wipe which increases the contact reliability. The modeled thermal and electrical behavior of the contacts is in good agreement with the experiments.

While the architecture of two series air gaps halves the required actuation stroke, the same architecture is prone to uneven mechanical loading and thus uneven contact resistance between the two air gaps which

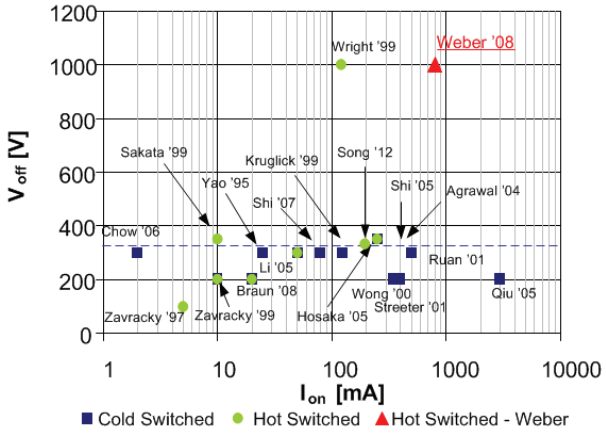

Figure 6. Voltage-standoff and current-carrying-capacity comparison of the MEMS relay here presented to those published in the literature.

limits ampacity. The uneven loading was reduced by adding torsional compliance to the moving contact. It could also be minimized through the use of a compliant contact design, i.e. that of a "wiffle-tree".

REFERENCES

[1] YH Song, et al, Proc. MEMS 2012, pp. 84-87.
[2] W Johler, IEEE TCPT, 27(1), 3/2004, pp. 19-29.
[3] HS Lee, et al, Sensors and Actuators A, 100(1), 2002, pp. 105-113.
[4] J Qiu, et al, JMEMS, 14(5):1099-1109, 2005.
[5] WP Taylor, JMEMS, 7(2):181-191, 1998.
[6] J Qiu, JMEMS, 13(2):137-146, 2004.
[7] SG Kim, in 18th. IEEE Conf. on MEMS, pp. 195-198, Miami, FL, 2005.
[8] JE Wong, et. al. MEMS 2000, Japan, pp. 633-638.
[9] H Hosaka, Sensors and Actuators, A , (40-1), Jan 1994, pp. 41-47.
[10] J Schimkat, Sensors and Actuators, 73(1999), pp. 138-143.
[11] AC Weber, in Proc. 2008 Solid-State Sensors, Actuators and Microsystems Workshop, pp. 52-53.
[12] AC Weber, et. al., IEEE 53rd Holm Conf., Sept. 2007, pp. 156-159.
[13] J Li, et. al., JMEMS, Vol. 14(6), 2005, pp. 1283-1297.
[14] SD Senturia. Micosystem Design. Kluwer Academic Publishers, 2000.
[15] R Holm. Electrical Contacts Theory and Appl.. Springer, Berlin, Germany, 4th ed., 1976.
[16] RS Timsit, IEEE TCPT, 22(1):85-98, 1999.
[17] AC Weber, Ph.D. thesis, MIT, 2008.
[18] M Read, et al, IEEE 56th Holm Conf., Oct 2010, pp. 1-8.